journal

J. Am. Ceram. Soc., 90 [2] 412–414 (2007)
DOI: 10.1111/j.1551-2916.2006.01424.x
© 2006 The American Ceramic Society

Synthesis of Nanosize-Necked Structure α- and γ-Fe_2O_3 and its Photocatalytic Activity

S. K. Apte, S. D. Naik, R. S. Sonawane, and B. B. Kale†

Centre For Materials For Electronics Technology (C-MET), Ministry of Information and Communication Technology, Goverment of India, Panchawati, Pune 411008 Maharashtra, India

J. O. Baeg

Advanced Chemical Division, Korea Research Institute of Chemical Technology, Daejon, South Korea

Highly dispersed nanometer-sized α-Fe_2O_3 (hematite) and γ-Fe_2O_3 (maghemite) iron oxide particles were synthesized by the combustion method. Ferric nitrate was used as a precursor. X-ray diffractometer study revealed the phase purity of α- and γ-Fe_2O_3. Both the products were characterized using field emission scanning electron microscope and transmission electron microscope for particle size and morphology. Necked structure particle morphology was observed for the first time in both the iron oxides. The particle size was observed in the range of 25–55 nm. Photodecomposition of H_2S for hydrogen generation was performed using α- and γ-Fe_2O_3. Good photocatalytic activity was obtained using α- and γ-Fe_2O_3 as photocatalysts under visible light irradiation.

I. Introduction

IRON oxide has been extensively studied in the past, owing to its wide applications as a pigment, in magnetic materials, and as catalysts and sensors.[1–5] The motivation for the fabrication of various morphologies and sizes of Fe_2O_3 nanoparticles was driven by the strong interest in their novel properties and potential application in electronics.[6–8] Major emphasis is given on magnetic recording applications-oriented materials. The unique magnetic properties of nanosized magnetic particles have made them potentially useful from both technological and theoretical points of view.[9] In the past, many synthesis methods have been developed for the preparation of α and hematite (γ-Fe_2O_3) including sol–gel, hydrolysis of iron salt, solvothermal, and hydrothermal synthesis.[7–10] As it is well understood that the electronic properties are dependent on particle morphology and size, recent research has been focused on the size and morphological control of iron oxide products.[7–11] The catalytic properties depend on the morphology, particle size, and surface area. In view of this, in the present study, we have synthesized a novel-necked structure nanosize α- and γ-Fe_2O_3 for the first time. Additionally, we have performed the photocatalytic activity of these iron oxides in H_2S splitting, i.e. hydrogen generation under visible light irradiation. The use of iron oxide as a photocatalyst has been given particular attention due to their absorption in the visible region, abundance, and low cost. Very limited literature is available[12,13] on the photocatalytic study of iron oxide. Therefore, we have studied the photocatalytic activity of necked structured nanosize iron oxide for the first time.

P. Gouma—contributing editor

Manuscript No. 21598. Received March 17, 2006; approved July 10, 2006.
†Author to whom correspondence should be addressed. e-mail: kbbb1@yahoo.com

II. Experimental Procedure

(1) Synthesis

Ferric nitrate, glycine, ammonium nitrate, and starch (Aldrich, Schnelldorf, Germany) were used in the synthesis of iron oxide. For the preparation of α-Fe_2O_3, ferric nitrate, glycine, and ammonium nitrate were taken in a stoichiometric mole ratio (1:1:1) and mixed thoroughly. The starch (0.1%–0.5%) was added in the above reaction mixture and homogenized, precisely. The reaction mixture (paste) was poured slowly in the combustion reactor at 550°, 600°, and 650°C and kept for 2 h. A very fine powder of α-Fe_2O_3 was obtained. Glycine was used as a combusting agent. For the preparation of γ-Fe_2O_3, α-Fe_2O_3 was further mixed with polyethylene glycol (PEG)–400 and combusted at 400°C for 2 h. Nanosize pure-phase γ-Fe_2O_3 was obtained. PEG added in this reaction system acts as an oxidant, surfactant, and dispersing agent. This ultimately prevents the particle agglomeration and results in the formation of high surface area free-flowing Fe_2O_3.

(2) Photodecomposition of H_2S

The photocatalyst was introduced as a suspension into a cylindrical Pyrex photochemical reactor with a quartz window and a thermostated water jacket. A Xe-lamp light source (Oriel, Newport Stratford, Stratford, CT) of intensity 450 W with a cut-off filter (>420 nm) was used. At a constant temperature of 25° ± 1°C, the vigorously stirred suspension was purged with argon for 1 h and then hydrogen sulfide (H_2S) was bubbled through the solution for about 1 h. Each experiment was carried out using 0.5 g of catalyst in 500 mL of KOH solution (0.5*M*) with a H_2S flow, 2.5 mL/min. The excess hydrogen sulfide was trapped in NaOH solution. The amount of evolved hydrogen was measured using graduated gas burette and a gas chromatograph (model Shimadzu GC-14B, Kyoto, Japan; MS-5 Å column, TCD, Ar carrier).

(3) Characterization

Powder X-ray diffractograms were recorded using an X-ray diffractometer (XRD, model Rigaku-D/Max-2200V, Tokyo, Japan) with Cu$K\propto$ radiation and a Ni filter. The surface morphology and particle size were determined using a field emission scanning electron microscope (FESEM model JEOL-JSM6700F, Tokyo, Japan) and transmission electron microscopy (TEM, model EF-TEM EM 912 Omega, Carl Zeiss (LeO), Oberkochen, Germany). Sonicated samples in ethanol were used for the TEM measurement. The spectroscopic study of the catalyst was carried out using a UV-visible (model Shimadzu UV-2450 diffuse reflectance model) spectrophotometer. Specific surface area measurements were performed using a BET surface area analyzer (model BET - Micromeritics ASAP-2400, Norcross, GA). FTIR (Spectrum—2000 Perkin Elmer, Wellesley, MA) was used to perceive the stretching of metal oxide bonding.

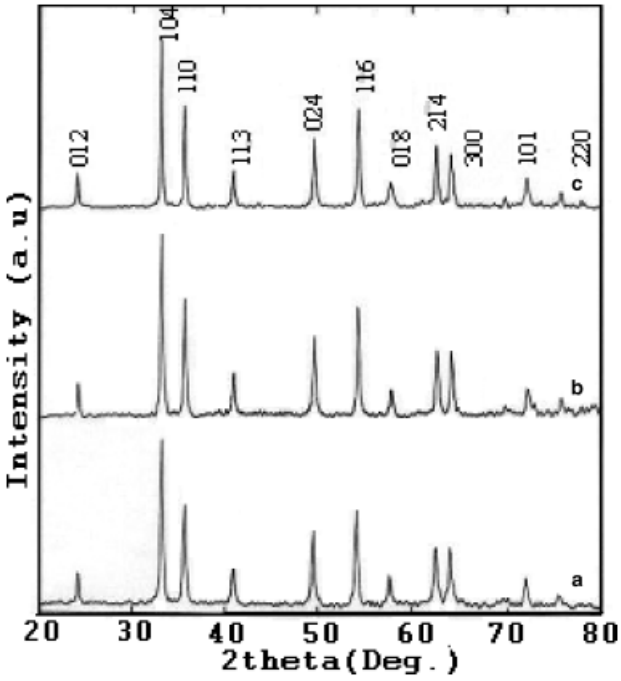

Fig. 1. X-ray diffractometer (XRD) pattern of hematite (α-Fe_2O_3).

III. Results and Discussion

(1) XRD Analysis

The α-Fe_2O_3 obtained at different temperatures was characterized using an XRD. Figures 1 (a)–(c) depict the XRD pattern of α-Fe_2O_3 prepared at 550°, 600°, and 650°C, respectively. The α-Fe_2O_3 diffraction peaks are identified, which are in good agreement with the reported values (JCPDS no. 33–363).[13] XRD data also revealed that the α-Fe_2O_3 obtained had an orthorhombic structure. There was no indication of any other additional phases, except α-Fe_2O_3 in the XRD pattern. It is also observed that the α-Fe_2O_3 is formed at 550°C itself. There was no appreciable change in structure at a higher temperature viz. 600° and 650°C, which indicates the good stability of α-Fe_2O_3.

Figure 2 shows the XRD pattern of γ-Fe_2O_3 prepared using PEG at 400°C. The diffraction peaks in the XRD pattern are in good agreement with the reported values given in the literature.[13] From the XRD data, it was observed that the XRD peaks of α- and γ-Fe_2O_3 show good broadening, indicating the ultra fine nature of the particles. The crystallite size calculated using Scherrer's equation is found to be 27 nm for α-Fe_2O_3 and 22 nm for γ-Fe_2O_3. The results are matching with the BET surface area of the α-Fe_2O_3 (61 m^2/g) and γ-Fe_2O_3 (68 m^2/g), respectively. There was no appreciable change in the particle size of α- and γ-Fe_2O_3.

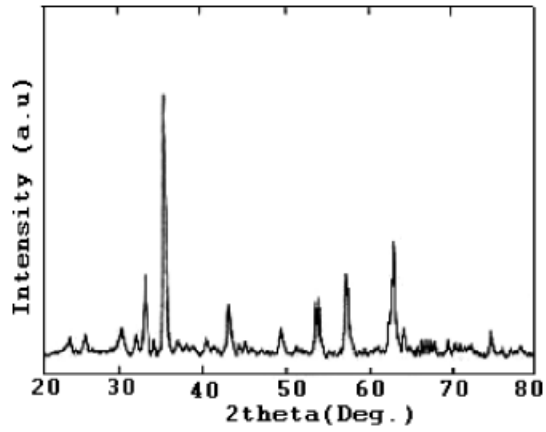

Fig. 2. X-ray diffractometer (XRD) pattern of maghemite (γ-Fe_2O_3).

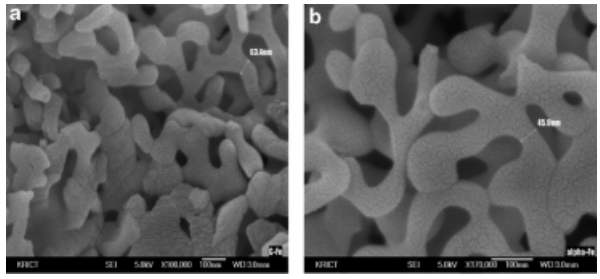

Fig. 3. Field emission scanning electron microscope (FESEM) image of (a) hematite (α-Fe_2O_3), (b) maghemite (γ-Fe_2O_3).

(2) Particle Morphology

Particle morphology of the samples was studied using FESEM. Figures 3(a) and (b) represents the FESEM micrographs of α-Fe_2O_3 and γ-Fe_2O_3, respectively. The necked structure morphology was observed in both the samples. Such type of a unique morphology was observed for the first time in iron oxide. The same samples were characterized using a TEM. Figures 4(a) and (b) depict the TEM images of α-Fe_2O_3 and γ-Fe_2O_3, respectively. TEM images clearly showed the micro-structural homogeneities and a remarkably unique necked structure morphology. FESEM and TEM pictures also show the nanocrystalline and porous nature of the product. From the FESEM and TEM, the particle size was observed to be in the range of 45–55 nm. There was no appreciable difference in the particle size of both the iron oxide samples, i.e., for α-Fe_2O_3 and γ-Fe_2O_3. FESEM and TEM images show that γ-Fe_2O_3 is slightly porous and smaller in size.

(3) Spectroscopic Analysis

Figures 5(a) and (b) represents the UV-visible diffused reflectance spectra of α-Fe_2O_3 and γ-Fe_2O_3, respectively. The absorption edge of both the samples is at 570–572 nm. The band gap estimated from the onset of the absorption edge was observed at 2.17–2.18 eV, which is in good agreement with a bandgap value of 2.2 eV for Fe_2O_3.[14] The steep absorption edge in both the samples is indicative of the uniform particle morphology and size with fairly good crystallinity.[15] A marginal shift in the absorption edge for γ-Fe_2O_3 may be due to slightly porous and small size-necked structure particles.[15]

Infrared spectroscopic studies were performed aimed to ascertain the metal oxygen nature of the product and to follow the dehydration process through the combustion technique. The FTIR of samples (a) and (b) are shown in Fig. 6. Sample (a) corresponds to α-Fe_2O_3 and (b) corresponds to γ-Fe_2O_3. Samples (a) and (b) showed absorption in the regions 3436, 1630, 1384, 532, 553, 458, and 442, and 374 cm^{-1}. The general range of 3600–3100 cm^{-1} (relating to antisymmetrical and symmetrical O–H stretching) may be assigned for water of hydration. Hydrates also absorb in the region of 1670–1600 cm^{-1} (relating to O–H bonding).[15] This latter bond can be taken as another important means of identifying water of crystallization and it has been found to be very useful in the elucidation of the crystal structure. In sample (a), the band associated with the lattice water molecule is broad and is observed in the region of 3436

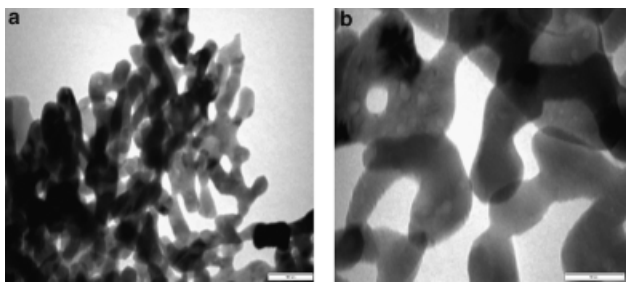

Fig. 4. Transmission electron microscopy (TEM) image of (a) hematite (α-Fe_2O_3), (b) maghemite (γ-Fe_2O_3).

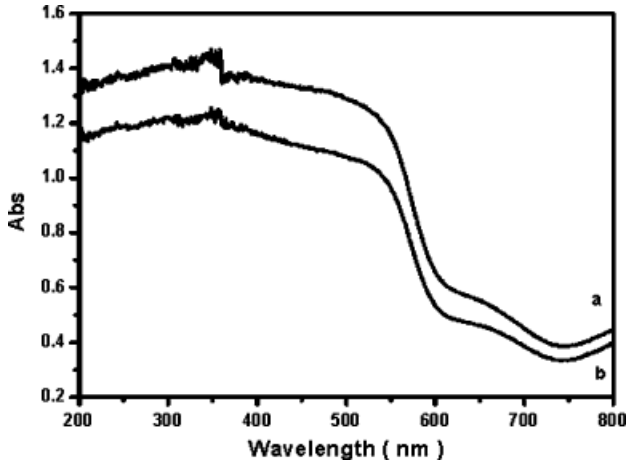

Fig. 5. UV-diffused reflectance spectra (DRS) spectrum of (a) hematite (α-Fe_2O_3), (b) maghemite (γ-Fe_2O_3).

and 1630 cm^{-1}. The simultaneous presence of these two bonds indicates that the water of crystallization is likely to be present in the sample. The same behavior was observed in sample (b), i.e., γ-Fe_2O_3. It is reported that the presence of water plays an important role in the formation and stabilization of γ-Fe_2O_3.[16] The bands at 458 and 432 cm^{-1} observed in sample (a) and at 442 and 553 cm^{-1} in sample (b) are due to metal oxygen stretching vibrational modes. These bands are intense and sharp. There was a slight shift in the γ-Fe_2O_3 because of absorbed oxygen and some amount of water being removed from γ-Fe_2O_3.[17] The intensity of the broad peaks at 3600–3000 cm^{-1} is found to be decreasing from samples (a) to (b). The shifts observed for the above samples may be due to the particle size effect.

(4) Photodecomposition of H_2S

The photocatalytic activity measurements for the hydrogen evolution from H_2S-splitting using α-Fe_2O_3 and γ-Fe_2O_3 under visible light irradiation show that both forms of iron oxide are photocatalytically active in the generation of hydrogen. An excellent photocatalytic activity was obtained for both forms of iron oxide. The maximum hydrogen generation rate achieved using necked nanosize α-Fe_2O_3 and γ-Fe_2O_3 was 50 mL/h and 51 mL/h, respectively. Their activities for the H_2 evolution under visible light irradiation are quite competitive.[18] The catalyst showed same activity after using it three times (8 h each). There is no report of hydrogen evolution from H_2S using α-Fe_2O_3 and

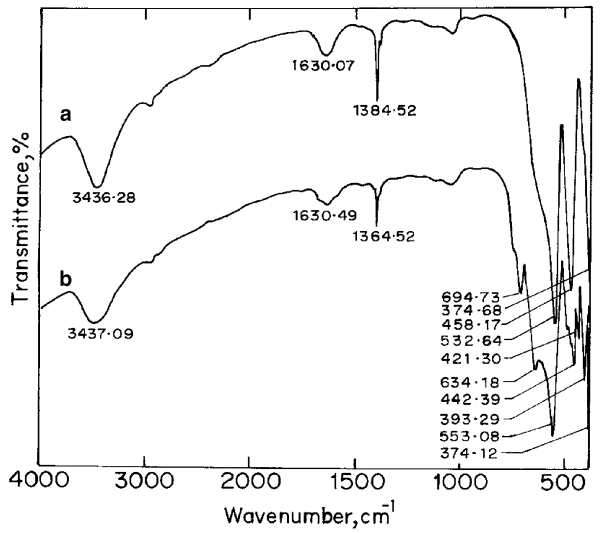

Fig. 6. Infrared (IR) spectrum of (a) hematite (α-Fe_2O_3), (b) maghemite (γ-Fe_2O_3).

γ-Fe_2O_3. However, we believe that α-Fe_2O_3 and γ-Fe_2O_3 may be showing good activity due to the nanosize porous and necked structure. Faust *et al.*[12] have already demonstrated the photocatalytic activity of α-Fe_2O_3 and concluded that surface hydroxyl groups as the principal reactive sites on the metal oxide surface are responsible for the photocatalytic activity. In the present case, the higher surface area and nanocrystalline-necked porous structure of α-Fe_2O_3 and γ-Fe_2O_3 further accelerate the photocatalytic activity. As iron oxide has a bandgap of 2.2 eV, it therefore absorbs solar radiation from 295 to 600 nm, which comprises 38% of the phonons of the solar spectrum. So, the photocatalytic activity obtained over a naked α-Fe_2O_3 and γ-Fe_2O_3 is quite explicable. Owing to the low cost of this catalyst. further work in this context related to parameters like stability, structure, and regeneration is under progress.

IV. Conclusion

Nanosize-necked structure α- and γ-Fe_2O_3 have been prepared from ferric nitrate by the combustion method. The α-Fe_2O_3 obtained has an orthorhombic structure, whereas γ-Fe_2O_3 has a tetragonal structure. The FESEM and TEM study revealed a unique necked structure with a particle size in the range of 45–55 nm. The BET surface area was observed to be in the range of 61–68 m^2/gm.

The steep absorption edge was observed at 572 nm (band gap, –2.18). α- and γ-Fe_2O_3 have shown good photocatalytic activity for hydrogen generation for H_2S under visible light irradiation. The maximum hydrogen production rate achieved was 50 mL/h for α-Fe_2O_3 and γ-Fe_2O_3.

References

[1]Q. Wang, H. Yang, J. Shi, and G. Zou, "One Step Synthesis of the Nanometer Particles of γ-Fe_2O_3 by Wire Electrical Explosion Method," *Mater. Res. Bull.*, **36**, 503–9 (2001).

[2]S. Kang, R. Subhash, F. R. John, and S. Pieter, "Synthesis and Characterization of Nanometer-Size Fe_3O_4 and γ-Fe_2O_3 Particles," *Chem. Mater.*, **8**, 2209–11 (1996).

[3]G. V. G. Reddy, K. Sheela, and S. V. Manorama, "Preparation of γ-Fe_2O_3 by the Hydrazine Method: Application as an Alcohol Sensor," *Int. J. Inorg. Mater.*, **2** [4] 301–7 (2000).

[4]K. Jung and C. Feldamann, "Non Agglomerated Sub-Micron-Fe_2O_3 Particles: Preparation and Applications," *J. Mater. Res.*, **15**, 2224–8 (2000).

[5]S. T. Aruna, S. Gosh, and K. C. Patil, "Combustion Synthesis and Properties of $Ce_{1-x}Pr_xO_{2-\delta}$ Red Ceramic Pigmets," *Int. J. Inorg. Mater.*, **3**, 387–92 (2001).

[6]Z. Jing, S. Wu, S. Zhang, and W. Huang, "Hydrothermal Fabrication of Various Morphological α-Fe_2O_3 Nanoparticles Modified by Surfactants," *Mater. Res. Bull.*, **39**, 2057–64 (2004).

[7]H. T. Sun, C. Cantalini, M. Faccio, M. Pelino, M. Cantalano, and L. Trapfer, "Porous Silica Coated α-Fe_2O_3 Ceramics for Humidity Measurement at Elevated Temperature," *J. Am. Ceram. Soc.*, **79** [4] 927–37 (1996).

[8]T. Hyeon, S. Lee, J. Park, Y. Chung, and H. B. Na, "Synthesis of Highly Crystalline and Monodisperse Maghemite Nanocrystalline Without a Size Selection Process," *J. Am. Chem. Soc.*, **123**, 12798–801 (2001).

[9]J. Fang, A. Kumbhar, W. L. Zhou, and K. L. Stokes, "Nanoneedles of Maghemite Iron Oxide Prepared From a Wet Chemical Route," *Mater. Res. Bull.*, **38**, 461–7 (2003).

[10]G. Sha, T. Wang, J. Xiao, and C. Liang, "A Mild Solvothermal Route to α-Fe_2O_3 Particles," *Mater. Res. Bull.*, **39**, 1917–21 (2004).

[11]J. Qiu, R. Yang, M. Li, and N. Jiang, "Preparation and Characterization of Porous Ultra Fine Fe_2O_3 Particles," *Mater. Res. Bull.*, **40**, 1968–75 (2005).

[12]B. C. Faust, M. R. Hoffmann, and D. W. Bahnemann, "Photocatalytic Oxidation of Sulfur Dioxide in Aqueous Suspension of Fe_2O_3," *J. Phy. Chem.*, **93**, 6371–81 (1989).

[13]C. Koramnn, D. W. Bahnemann, and M. R. Hoffmann, "Environmental Photochemistry: Is Iron Oxide (Hematite) an Active Photocatalyst? A Comparative Study: α-Fe_2O_3, ZnO, TiO_2," *J. Photoch. Photobio A: Chem.*, **48**, 161–9 (1989).

[14]W. B. Jr. Ingler and S. U. M Khan, "Photoresponse of Spray Pyrolytically Synthesized Copper–Doped p-Fe_2O_3 Thin Film Electrodes in Water Splitting," *Int. J. Hydrogen Energ.*, **30** [8] 821–5 (2005).

[15]H. Hsiang and F. S. Yen, "Effects of Mechanical Treatment on Phase Transformation and Sintering of Nano-Sized γ-Fe_2O_3 Powder," *Ceram. Int.*, **29**, 1 (2003).

[16]K. S. Rane and V. M. S. Vernekar, "Synthesis of Ferrite Grade γ-Fe_2O_3," *Bull. Mater. Sci.*, **24** [1] 39–45 (2001).

[17]A. Venkataraman, V. A. Hiremath, S. K. Date, and S. D. Kulkarni, "Combustion Route to γ-Fe_2O_3 Synthesis," *Bull. Mater. Sci.*, **24** [6] 617–21 (2001).

[18]A. Kudo, H. Kato, and I. Tsuji, "Strategies for the Development of Visible-Light Driven Photo Catalysts for Water Splitting," *Chem. Lett.*, **33** [12] 1534–6 (2004). □